SPREAD OF PLASTICITY: AN ADAPTIVE GRADUAL PLASTIC-HINGE APPROACH FOR STEEL FRAMES

Yanglin Gong
Department of Civil Engineering, Lakehead University, Thunder Bay, Ontario, Cnada P7B 5E1
E-mail: ygong@lakeheadu.ca

Abstract

This paper presents a new plastic-hinge method for inelastic analysis of steel frames. The proposed plastic-hinge model employed two parameters in the modeling. The first parameter involves mimicking the spread of plasticity through a section depth, while the second incorporates the spread of plasticity along a member length. Procedures to determine the key parameters are developed using moment-curvature-thrust relationship for steel beam-columns. The proposed analysis method is especially advantageous when modeling the spread of plasticity along a member length using various discretization schemes. Two numerical examples are performed to demonstrate the accuracy and simplicity of the method.

Keywords: steel frames, nonlinear analysis, plasticity, plastic-hinge, beam-columns

Introduction

Considerable studies have been undertaken on the inelastic analysis of steel frames in recent years (Chen and Toma 1994, Xu et al. 2005). The inelastic analysis methods are generally classified into two types: the distributed plasticity method and the plastic-hinge method. The distributed plasticity method discretizes frame members both along their length and through their cross section into many elements. The spread of plasticity is traced by the sequential yielding of the elements. This method is usually adopted to create benchmark solutions, as it is too computationally intensive and not suitable for practical design purposes. On the contrary, the plastic-hinge method usually involves using single or multiple elements to model a frame member, thus making it more efficient and the preferred method in engineering practice. The plastic-hinge method assumes that inelastic deformations are concentrated at plastic hinges at the end of elastic elements. The early studies used an elastic-plastic-hinge model, where the relationship between moment and curvature is linear up to the full plastic-moment of a section, after which the section becomes a perfect hinge. Though this approach is easy to implement, it often overestimates the ultimate strength of structural systems. More recently, refined- and quasi-plastic-hinge approaches (Liew et al. 1993, Attalla et al. 1994) with two-surface yielding criteria were proposed to account for the gradual plastification within steel members. Often, a model was constructed to simulate the gradual softening of plastic-hinges whose force point falls within the two yielding surfaces (Chen and Chan 1995, Hasan et al. 2002, Xu et al. 2005, Xu and Liu 2005).

This study proposes a new gradual plastic-hinge model for the inelastic analysis of planar steel frames. The analysis approach belongs to the domain of matrix displacement method. The plastic-hinge model is capable of mimicking the spread of plasticity both through the depth of a section and along the length of an element. The moment gradient of a frame member is directly taken into account in the plastic-hinge model. The model is unique and applicable to a general steel beam-column.

In this study, it is assumed that the cross sections are doubly symmetric and the stress-strain relation for steel material is elastic-perfectly-plastic. Only moment yielding is considered, while shear and axial yielding are ignored. Local plate, torsional, and lateral-torsional buckling are not considered.

Inelastic Beam-Column Model

A hybrid element (see Fig.1) is employed to model planar inelastic beam-columns. The element consists of two potential plastic-hinges at the ends of an elastic beam-column. Each plastic-hinge is modeled by a nonlinear zero-length rotational spring (which is called a hinge-spring or spring hereafter). For the elastic beam-column, E, I, and A correspond to Young's modulus, moment of

M. Pandey et al. (eds), Advances in Engineering Structures, Mechanics & Construction, 265–276.

inertia, and cross-sectional area of the element. All the plastification is assumed to be concentrated at end plastic-hinges.

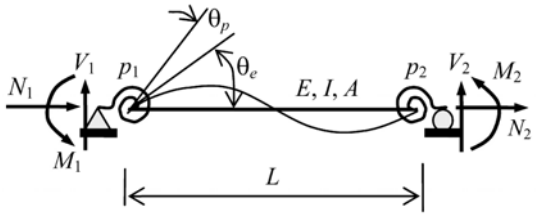

Fig. 1 Hybrid beam-column element and its end rotation

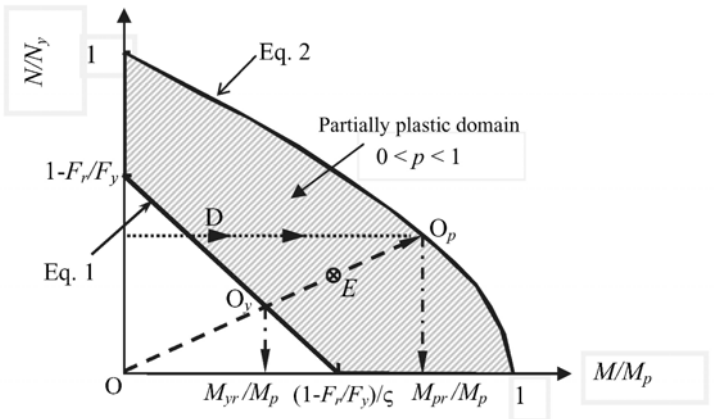

Fig. 2 Yielding criteria under combined axial force and bending moment

The interaction between the axial force N and moment M is considered using a two-surface criterion, as shown in Fig. 2. For the first-yield surface, the equation is

$$M/M_y + N/N_y = 1 - F_r/F_y \tag{1}$$

where: $M_y=F_y S$ is the first-yield moment of the section under a pure moment and S is the elastic modulus of the cross section; $N_y=AF_y$ is fully-plastic axial force capacity under a pure axial force; F_y is yielding stress of steel; and F_r is the peak residual stress in the flange of cross-section. In the meantime, the full-yield surface is expressed as

$$M/M_p + \left(N/N_y\right)^a = 1 \tag{2}$$

where $M_p=F_y Z$ is the plastic moment of the section under a pure moment and Z is the plastic modulus; and the exponent a depends on the shape of the section. For example, a=1.3 for a wide-flange section under strong axis bending (Duan and Chen 1990). Therefore, any section having a force point falling within the shaded area is partially yielded (see Fig. 2).

Adaptive Gradual Plastic-Hinge Model

To assign a plasticity-factor p (see Eq. 8 for definition) to a partially-yielded section (e.g., a section with force point E in Fig. 2) during a loading process, it is assumed that the ratio M/N for the section remains invariant when $M\neq 0$ (see line O-O_y-E-O_p in Fig. 2. O_y and O_p thus represent the first-yield and full-yield 'times' for the section, respectively.). Defining $\xi=(M_p/N_y)(N/M)$, the reduced first-

yield moment M_{yr} for the section in post-elastic range under combined axial force and bending moment is

$$M_{yr} = M_y \left(1 - F_r / F_y\right) / \left(1 + \xi / \varsigma\right) \tag{3}$$

where $\varsigma = Z/S$ is shape factor. The reduced full-yield moment M_{pr} is found from Eq. 2 as

$$M_{pr} / M_p + \left(\xi M_{pr} / M_p\right)^a = 1 \tag{4}$$

Note that the assumption of N/M as invariant is not necessarily true. This assumption purely serves the purpose of evaluating the plasticity-factor for a partially yielded hinge.

The rotational stiffness of a hinge-spring degrades from infinity to zero as the moment M at the hinge section increases from M_{yr} to M_{pr}. This degradation is represented by a moment-plastic rotation curve (see Fig. 3). On this curve, point $(0, M_{yr})$ corresponds to the first-yield of the hinge, while point (θ_{pu}, M_{pr}) corresponds to the full-yield. This curve is expressed as (Xu et al. 2005)

$$\left(\frac{M - M_{yr}}{M_{pr} - M_{yr}}\right)^{\eta} + \left(\frac{\theta_{pu} - \theta_p}{\theta_{pu}}\right)^{\eta} = 1 \qquad (\theta_p < \theta_{pu}, M_{yr} < M < M_{pr}) \tag{5}$$

where θ_{pu} is the plastic rotation at which the hinge-spring has zero stiffness; and exponent η is a parameter dependent on the shape of the cross-section. Upon differentiating moment M with respect to plastic rotation θ_p in Eq. 5, the instantaneous rotational stiffness of the hinge-spring is found as

$$R_m = \frac{dM}{d\theta_p} = \frac{M_{pr} - M_{yr}}{\theta_{pu}} \left(1 - \frac{\theta_p}{\theta_{pu}}\right)^{\eta - 1} \left[1 - \left(1 - \frac{\theta_p}{\theta_{pu}}\right)^{\eta}\right]^{\frac{1}{\eta} - 1} \qquad (0 < \theta_p < \theta_{pu}) \tag{6}$$

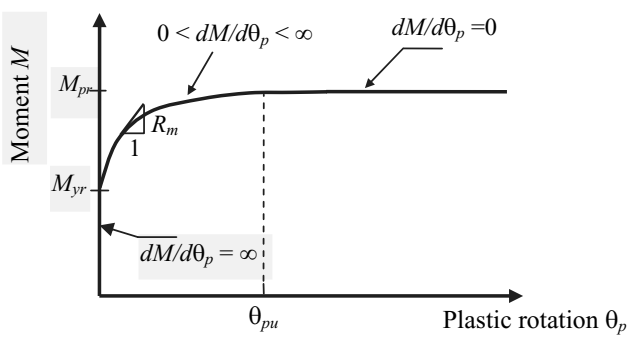

Fig. 3 Moment-plastic rotation curve of plastic-hinges

Equation 6 can be rewritten as

$$R_m = \frac{M_{pr} - M_{yr}}{\theta_{pu}} \left[1 - \left(\frac{M - M_{yr}}{M_{pr} - M_{yr}}\right)^{\eta}\right]^{\frac{\eta - 1}{\eta}} \left(\frac{M - M_{yr}}{M_{pr} - M_{yr}}\right)^{1 - \eta} \qquad (M_{yr} < M < M_{pr}) \tag{7}$$

Then, the plasticity-factor p for a plastic-hinge is defined as

$$p = \frac{\Delta\theta_e}{\Delta\theta_e + \Delta\theta_p} = \frac{1}{1 + 3EI/R_m L} \tag{8}$$

where: $\Delta\theta_e = \Delta M \bullet L/3EI$ is the incremental end rotation of the elastic beam-column (see Fig.1); ΔM is a moment increment; and $\Delta\theta_p = \Delta M/R_m$ is the incremental rotation of the spring. For a fully elastic section $R_m = \infty$ and $p=1$, for a fully plastic hinge $R_m=0$ and $p=0$, while for a partially plastic hinge $0<p<1$.

Upon introducing the plasticity-factor by Eq. 8, the stiffness matrix $\mathbf{K}_e$ for the hybrid element in Fig.1 is found as (Xu 2001, Hasan et al. 2002),

$$\mathbf{K}_e = \mathbf{S}\,\mathbf{C}_s + \mathbf{G}\,\mathbf{C}_g \tag{9}$$

where: $\mathbf{S}$ is the standard stiffness matrix for an elastic frame member; $\mathbf{C}_s$ is a correction matrix expressed in terms of plasticity-factors p (Hasan et al. 2002); $\mathbf{G}$ is the standard geometric stiffness matrix; and $\mathbf{C}_g$ is the corresponding correction matrix formulated as a function of p (Hasan et al. 2002).

A unique feature of the stiffness matrix $\mathbf{K}_e$ is that the stiffness of the springs R_m is not directly included in Eq. 9. Instead, the contribution of the hinge-springs to the element stiffness is incorporated through the plasticity-factors p. Such a treatment for R_m significantly improves the accuracy of the element model. To explain this, the R_m-M curves (see Eq. 7) and the corresponding p-M curves for an element of W200×46 section (CISC 2004) are drawn in Figs. 4 and 5, respectively. From Fig. 4, it is seen that spring stiffness R_m is extremely sensitive to moment M in the early post-elastic range. The stiffness R_m is infinite when $M=M_{yr}$, then R_m dramatically drops as M begins to exceed M_{yr}. R_m is also very sensitive to slight variations in parameter η. For instance, R_m=166323 kN-m/radian for η=1.8 under $M=1.03M_{yr}$, which is 2.5 times of that for η=1.5 under the same moment. This high sensitivity of R_m to M and η can be interpreted as a difficulty in modeling R_m numerically since some approximation in the R_m model is generally unavoidable. Therefore, if R_m is directly included in the stiffness matrix, considerable errors may be introduced. On the contrary, the plasticity-factor p has a relatively even degradation rate with the increasing of M, as shown in Fig. 5. Thus, some inaccuracy in R_m model does not cause much error in p value. Therefore plasticity-factor p serves as an 'error filter' in the hinge model.

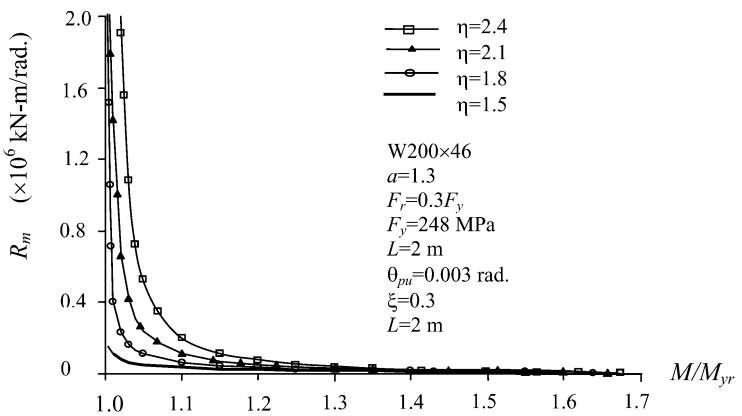

Fig. 4 Relations between moment and stiffness of hinge-spring

There are two key parameters, η and θ_{pu}, in the hinge-spring model Eq. 7. This study makes full use of these two parameters by employing η to simulate the spread of plasticity through the depth of a cross section and θ_{pu} to mimic the spread of plasticity along the length of an element.

It is obvious that parameter η has a significant impact on the degradation rate of the spring stiffness. For instance, the spring having η=1.8 degrades faster than the spring having η=2.1 (see Fig.5). In fact, this variation in degradation rate reflects the geometric difference among various cross sections. For example, an I-section degrades faster than a rectangular section under bending since an I-section has more materials allocated away from its neutral axis than a rectangular section has. Thus, the determination of η value is dependent on the shape of cross section. As it is shown in the numerical examples, η is taken as 1.8 for wide flange I-sections (and it was calibrated with experimental results). It appears that η=2.1 is reasonable for a rectangular section and η=2.4 for a solid circular section. By determining the η value in such a way one can simulate the spread of plasticity through a cross section.

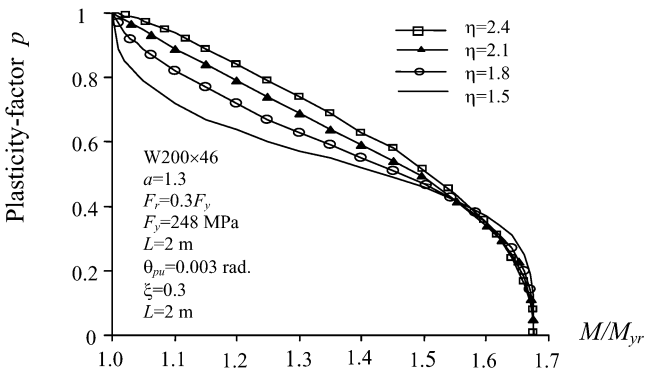

Fig. 5 Relations between moment and plasticity-factor

Before determining parameter θ_{pu}, it is instructive to examine how θ_{pu} affects the plasticity-factor of a hinge-spring. The relations between p and M for different θ_{pu} values are presented in Fig. 6 for the same element of W200×46 section. Figure 6 clearly illustrates that a larger θ_{pu} value will result in a softer hinge-spring. When θ_{pu} value is very small, the hinge-spring behavior is approaching that of a conventional elastic-plastic-hinge.

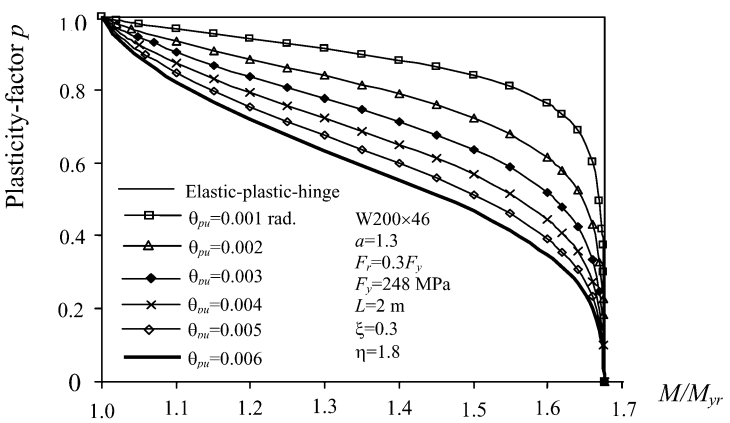

Fig. 6 Relations between plasticity-factor and θ_{pu}

To simulate the spread of plasticity along the length of a member, the parameter θ_{pu} must consider the distribution of bending moment along the length of the member (called moment gradient). In the following, the moment-curvature-thrust relations for beam-columns will be reviewed first, and then θ_{pu} value will be computed considering different moment gradients.

Moment-Curvature-Thrust Curves (*M*–ϕ–*N*) of Beam-Columns

The moment-curvature-thrust curves for general beam-columns were given by Chen (1971). A typical presentation of these curves is shown in Fig. 7, where the curvature is normalized by ϕ_y ($\phi_y=2\varepsilon_y/d$, where d=depth of a section, $\varepsilon_y=F_y/E$). According to Chen (1971), it needs two functions to represent M-ϕ relation in the post-elastic range.

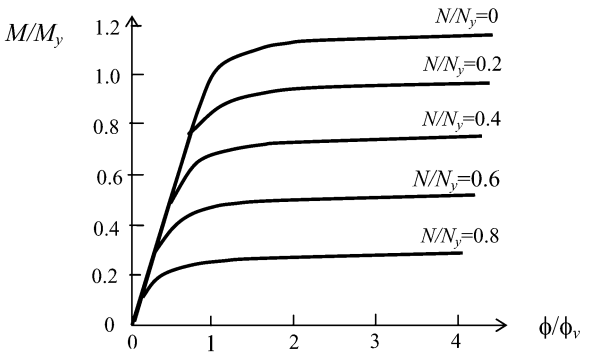

Fig. 7 Moment-curvature-thrust curves

In this study, the moment-curvature-thrust curves in Fig. 7 are expressed approximately as a unified form as shown in Fig. 8a. In the elastic range ($M \le M_{yc}$, where M_{yc} is the first-yield moment allowing for axial force), $\phi=M/EI$ (and $\phi_{yc}=M_{yc}/EI$ at the first-yield). After $M>M_{yc}$, M-ϕ relation becomes nonlinear, and $\phi=\phi_e+\phi_p$ (ϕ= total curvature, ϕ_e=elastic curvature, and ϕ_p=plastic curvature). The section is approximately fully yielded at curvature ϕ_{fu}, where ϕ_{fu} can be expressed as a constant ω_1 multiplied by ϕ_{pc} ($\phi_{pc}=M_{pc}/EI$, where M_{pc} is the full-yield moment allowing for axial force). Note that the determination of moments M_{yc} and M_{pc} does not involve the assumption of M/N being constant (hence different symbols are used). From Eqs. 1 and 2, we have

$$M_{yc} = M_y\left(1 - F_r/F_y - N/N_y\right) \tag{10}$$

$$M_{pc} = M_p\left(1 - \left(N/N_y\right)^a\right) = \varsigma M_y\left(1 - \left(N/N_y\right)^a\right) \tag{11}$$

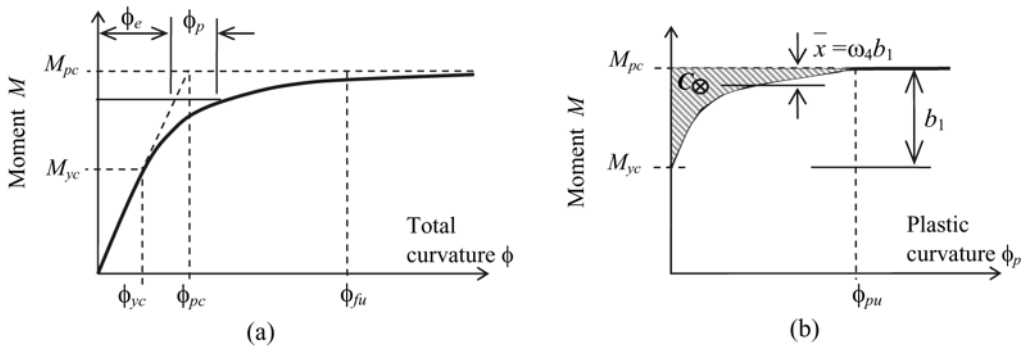

Fig. 8 Moment-curvature relationships: (a) total curvature (b) plastic curvature

For I-sections bending about strong axis, ω_1=1.9. The corresponding moment is found to have an average value of 96% of M_{pc} for $0\le N/N_y\le 0.6$ (Chen 1971). The plastic curvature at the onset of full-yield is approximately equal to $\phi_{pu}=\phi_{fu}-\phi_{pc}=(\omega_1-1)\phi_{pc}=\omega_2\,\phi_{pc}$. For applying M-ϕ_p relation later in this

study, the shaded area to the left of the curve (see Fig. 8b) can be found to be ($\omega_3 \times \phi_{pu} \times b_1$) and the centroid of the shaded area to the $M=M_{pc}$ line is $\bar{x} = \omega_4 b_1$. From Fig. 8a, we have

$$\phi_{pu} = \omega_2 \left(M_{pc}/EI\right) = \left(\omega_2/EI\right)\varsigma SF_y \left[1-\left(N/N_y\right)^a\right] = \left(2\omega_2 \varepsilon_y \varsigma/d\right)\left[1-\left(N/N_y\right)^a\right] \tag{12}$$

where: $\varepsilon_y = F_y/E$, $I/S = d/2$, and d=depth of a cross section.

Computation of Parameter θ_{pu}

For the hybrid element, the total rotation θ at an end is comprised of two parts (see Fig. 1). The first part, θ_e, represents the end rotation of the elastic beam-column, while θ_p represents the plastic rotation of the hinge. Thus, at the full-yield $\theta = \theta_e + \theta_{pu}$. To simulate the spread of plasticity of an actual inelastic beam-column, the θ of the hybrid element must be identical to that of an actual beam-column.

Consider an actual inelastic beam-column under linear distributed first-order moments (see Fig. 9a). Define moment gradient $\kappa = \pm|M_2/M_1|$, where M_2 and M_1 are the bending moments at Ends 1 and 2, respectively, and $M_2 \le M_1$. Moment gradient κ is positive for double curvature and negative for single curvature ($-1 \le \kappa \le 1$). The lengths of the plastic zones at Ends 1 and 2 are L_1 and L_2, respectively. The corresponding curvature distribution along the member is illustrated in Fig. 9b. The plastic curvature begins at the section where moment is equal to M_{yc}. Figure 9c shows the distribution of plastic curvature alone at the onset of full-yield at End 1. Note that the identical relationship between M and ϕ_p at End 1 and in Fig. 8b. Amongst the total rotation End 1 undergoes, the portion of plastic rotation comes from the plastic curvatures along the length of the member. Assume that θ_{pu} of the hinge-spring is equal to the plastic rotation θ_p at End 1when the end is at the onset of full-yield.

The conjugate beam method is used to evaluate the plastic rotation at End 1 for the beam-column under a curvature loading shown in Fig. 9c. The conjugate beam is under the loading of plastic curvatures alone since only plastic rotation is of concern. The end rotation of the actual beam-column is equal to the shear at the same section of its conjugate beam.

For calculating θ_{pu}, moments M_{yc} and M_{pc} shall be computed from Eqs. 10 and 11, respectively. This can be seen clearly from the fact that the load path from the section with zero moment along the member length to End 1 follows line D-O_p in Fig. 2 (N remains unchanged along the member length).

It is desirable to correlate θ_{pu} to the moment gradient κ because plastic zones within a member are dependent on the moment distribution along the length (see Fig. 9a). In the following θ_{pu} values corresponding to four particular moment gradient κ are determined first. Then, the interpolation method is used to compute θ_{pu} value for any moment gradient κ.

For the convenience of deriving formulations for θ_{pu}, the ratio γ is defined as

$$\gamma = M_{yc}/M_{pc} = \frac{1 - F_r/F_y - N/N_y}{\varsigma\left(1-\left(N/N_y\right)^a\right)} \tag{13}$$

Then, θ_{pu} values corresponding to four different moment gradient κ are found as follows:

(1) κ=1, double curvature. $M_1 = M_2 = M_{pc}$ and $\phi_p = \phi_{pu}$ at both end sections. The lengths of plastic zones are $L_1 = L_2 = 0.5(1-\gamma)L$. The centroid of curvature loading at each end is $\bar{x} = \omega_4 L_1$, while the area of plastic curvature loading at each end is equal to ($\omega_3 \times \phi_{pu} \times L_1$). Therefore, the shear force at End 1 of the conjugate beam under the plastic curvature loading is equal to

$$\theta_{pu} = \omega_3 \phi_{pu} L_1 \left(L - 2\bar{x}\right)/L = \omega_2 \omega_3 \varsigma \varepsilon_y (1-\gamma)\left[1-\omega_4(1-\gamma)\right]\left[1-\left(N/N_y\right)^a\right](L/d) \quad (\kappa=1) \tag{14}$$

(2) κ=0, single curvature. $M_1 = M_{pc}$ and $\phi_p = \phi_{pu}$ at End 1, while $M_2 = 0$ and $\phi_p = 0$ at End 2. Plastic zones are $L_1 = (1-\gamma)L$ at End 1 and $L_2 = 0$ at End 2. Hence, the shear force at End 1 of the conjugate beam under the plastic curvature loading is equal to

$$\theta_{pu} = \omega_3 \phi_{pu} L_1 \left(L - \bar{x}\right) / L = 2\omega_2 \omega_3 \varsigma \varepsilon_y (1-\gamma)\left[1 - \omega_4 (1-\gamma)\right]\left[1 - \left(N/N_y\right)^a\right](L/d) \quad (\kappa=0) \qquad (15)$$

(3) $\kappa = -\lambda$, single curvature. $M_1=M_{pc}$ and $\phi_p = \phi_{pu}$ at End 1, and $M_2=M_{yc}$ and $\phi_p=0$ at End 2. Then $L_1=L$ at End 1 and $L_2=0$ at End 2. The shear force at End 1 of the conjugate beam under the plastic curvature loading is equal to

$$\theta_{pu} = \omega_3 \phi_{pu} L \left(L - \bar{x}\right) / L = 2\omega_2 \omega_3 (1-\omega_4) \varsigma \varepsilon_y \left[1 - \left(N/N_y\right)^a\right](L/d) \quad (\kappa = -\lambda) \qquad (16)$$

(4) $\kappa = -1$, single curvature. $M_1=M_2=M_{pc}$ and $\phi_p=\phi_{pu}$ along the length of the member. The conjugate beam is under uniform plastic curvature loading. The shear force at the end of the conjugate beam is

$$\theta_{pu} = \phi_{pu} L/2 = \omega_2 \varsigma \varepsilon_y \left[1 - \left(N/N_y\right)^a\right](L/d) \quad (\kappa = -1) \qquad (17)$$

Equations 14 to 17 are for a general beam-column. The factors ω_2, ω_3, ω_4, a, ς, and γ are dependent on the sectional properties of the beam-column.

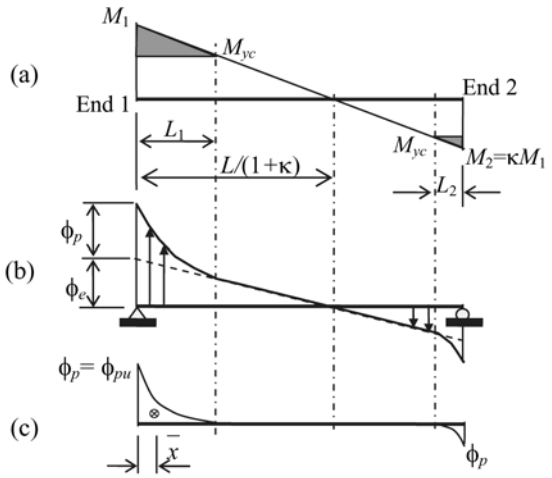

Fig. 9 Conjugate beam method for computing end rotation: (a) linear moment distribution and plastic zones (b) total curvature distribution and curvature loading for conjugate beam (c) plastic curvature distribution when End 1 is at the incipience of full-yield.

I-Sections

This section is to illustrate how to use Eqs. 14 through 17 to determine θ_{pu}-κ relation for wide flange I-sections bending about strong axis (i.e. W-sections in CISC 2004). For W-sections: it is found that $\omega_2=0.9$, $\omega_3=0.308$, and $\omega_4=0.21$ using the moment-curvature-thrust curves given by Chen (1971); the average section shape factor $\varsigma = 1.14$; the peak residual stress is commonly taken to be 30% of yielding strength (i.e., $F_r=0.3F_y$).

It is found that θ_{pu} is not sensitive to N/N_y ratios when $\kappa=1$ and 0. Thus, Eqs. 16 and 17 are simplified respectively for W-sections as

$$\theta_{pu} = 0.116\, \varepsilon_y (L/d) \quad (\kappa=1) \qquad (18)$$

$$\theta_{pu} = 0.233\, \varepsilon_y (L/d) \quad (\kappa=0) \qquad (19)$$

Assuming a moderate axial force N=0.2N_y for a general beam-column, then $\varsigma\,[1-(N/N_y)^a]=1.0$ in Eqs. 16 and 17, which are respectively simplified as

$$\theta_{pu}=0.438\varepsilon_y(L/d)\quad(\kappa=-0.5) \tag{20}$$

$$\theta_{pu}=0.9\varepsilon_y(L/d)\quad(\kappa=-1) \tag{21}$$

Based on Eqs. 18 through 21, a piecewise θ_{pu}-κ curve is established for W-sections in Fig. 10. Using the interpolation method, a unique θ_{pu} value is available corresponding to the κ value of an element. The moment gradient κ of an element at the first-yield of one hinge-spring is used to determine the θ_{pu} value for that spring. After the θ_{pu} value is computed for a particular hinge-spring, its value will remain unchanged during the rest of the loading history.

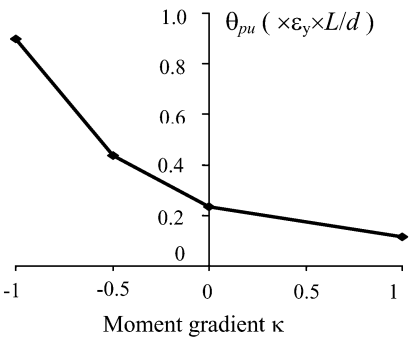

Fig. 10 Relation between moment gradient κ and θ_{pu} value for W-sections

Analysis Procedures

Incremental single-step method, as described in the following, is employed to conduct nonlinear analysis for steel frameworks.

1) Discretize frame members into elements. Initialize plasticity-factors to be p_1=p_2=1 for all elements.
2) Form element stiffness matrix $\mathbf{K}_e$ for each element, which involves using plasticity-factors from previous loading step to compute $\mathbf{C}_s$ and $\mathbf{C}_g$ (p=1 for the first loading step). Then assemble overall structure stiffness matrix **K**. If the tangent stiffness matrix **K** is found to be singular, which indicates the structure collapses, terminate analysis.
3) Solve for incremental nodal displacements by $\Delta\mathbf{F}=\mathbf{K}\bullet\Delta\mathbf{u}$, where **u** and **F** are the vectors of overall nodal displacements and loads respectively. Calculate incremental deformations and forces for each element. Update the total overall nodal displacements and loads, and member internal forces by $\mathbf{u}=\sum\Delta\mathbf{u}$, $\mathbf{F}=\sum\Delta\mathbf{F}$, and $\mathbf{f}_j=\sum\Delta\mathbf{f}_j$, respectively, where $\mathbf{f}_j$ is the vector of member internal force.
4) Check the yielding status for each hinge-spring at the ends of each element. The combined actions of axial force and bending moment at a hinge-spring are, from Eqs. 1 and 2, denoted as $\beta_1=M/M_y+N/N_y$ and $\beta_2=M/M_p+(N/N_y)^a$. Then update p for each spring as below:
   (i) If $\beta_1\le(1-F_r/F_y)$, the hinge-spring is still fully elastic with p=1.
   (ii) If $\beta_1>(1-F_r/F_y)$ and $\beta_2<1$, the hinge-spring is partially plastic. Calculate M_{yr} and M_{pr} from Eqs. 3 and 4, respectively. If the hinge-spring is found to be yielding for the first time, calculate its θ_{pu} value using θ_{pu}-κ relation. Compute the post-elastic rotational stiffness of the hinge-spring from Eq. 7 and the plasticity-factor p from Eq. 8.
   (iii) If $\beta_2\ge1$, the hinge-spring is fully plastic with p=0.
5) Go back to step 2.

Numerical Examples

The inelastic analysis is illustrated for two structures comprised of steel members of wide flange I-section. All the members are oriented with their webs in the loading plane. The exponent η in Eq. 5 is taken as 1.8. Young's modulus is E=2×10^5 MPa.

Example 1: A Simply-Supported Beam

The first example is a simply-supported beam (see Fig. 11), which was tested by Lay and Galambos (1964). The section is W130×28, with the measured properties being A=3606 mm^2, I=11.16×10^6 mm^4, S=168.8×10^3 mm^3, Z=190.1×10^3 mm^3, d=132 mm, F_y=247 MPa, and F_r = 19.8 MPa. $M_p = Z \times F_y$ = 47 kN-m, and load capacity P=71 kN. Equations 14 to 17 are used to establish θ_{pu}-κ relation for this beam. ω_2=0.9, ω_3=0.308 and ω_4=0.21.

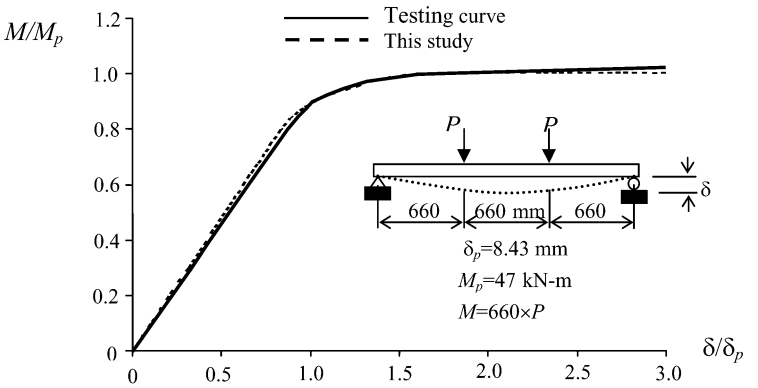

Fig. 11 Moment-deflection curve of the simply-supported beam

The middle portion of this beam is a region of constant moment. This entire region begins to yield when its moment exceeds the first-yield moment. Therefore, this beam is of particular interest for this study since the wide spread of plasticity both through the depth of the section and along the length of the beam took place. Such a structure with a large plastic zone is generally regarded as being difficult for a plastic-hinge method to model.

First, the beam was analysed by using four elements, as shown in Fig. 12b where the digit inside a rectangular box represents the element number. The middle portion is represented by two identical elements 2 and 3. The moment-deflection curve at midspan section is drawn in Fig. 11. Compared with the test curve, the errors of the theoretical analysis are within 5%. Next, the beam was re-analysed using a 3-element discretization scheme (see Fig. 12a). Table 1 records the θ_{pu} value for hinge-springs of different discretization schemes. The deflection at the one-third point at the incipience of collapse is also recorded in Table 1. The plasticity-factors under 90% of the collapse load are depicted in Fig. 12, where an oval represents a hinge-spring and the number inscribed in it is the corresponding plasticity-factor p.

Table 1 Analysis of the simply-supported beam using different discretization schemes

Discretization scheme	θ_{pu} for hinge-springs			Deflection at one-third point at collapse (mm)
	Element 1	Element 2	Element 3	
3-element	0.00068	0.00626	0.00068	11.723
4-element	0.00068	0.00313	0.00313	11.723

For the 3-element scheme, Table 1 shows that the θ_{pu} value for the hinge-springs of element 2 is 9.2 times as large as that for the hinge-springs of elements 1 and 3. Therefore, the hinge-springs of element 2 have a significantly smaller p value (i.e., p_1=p_2=0.18) than the hinge-springs of elements 1 (p_2=0.67) and 3 (p_1=0.67) as illustrated in Fig. 12a, even though all these hinge-springs are subjected

to an identical moment. This substantially smaller p value for element 2 is translated into a much smaller stiffness for the middle portion of the beam, which is in keeping with the fact that the entire middle portion is a plastic zone. Thus, the parameter θ_{pu} is capable of imitating the spread of plasticity along the length of a member.

It is noted from Table 1 that the two analyses obtain identical deflection. It is further noted from Figs. 12a and 12b that the plasticity-factors are identical for these two discretization schemes. The two discretization schemes have identical beam stiffness at every loading step. This can be explained by inspecting Eqs. 7 and 8 and θ_{pu} values in the table. The θ_{pu} value for elements 2 and 3 of the 4-element scheme is half of that for element 2 of the 3-element scheme (θ_{pu} is proportional to element length L. The elements in the middle portion have $\kappa = -1$). Hence, the product $R_m L$ in Eq. 8 remains unchanged whether the middle portion of the beam is represented by one or two (or more) elements.

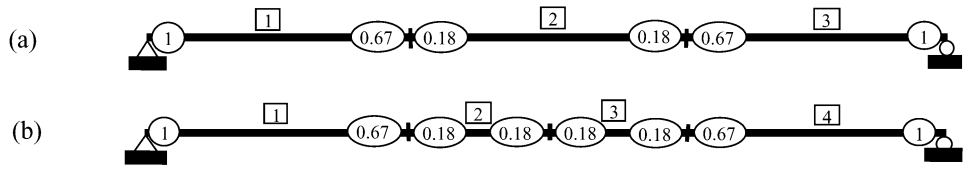

Fig.12 Plasticity-factors for two discretization schemes at $M=0.9M_p$: (a) 3-element, (b) 4-element

Example 2: A 2-Story Moment Frame

Consider the steel frame subjected to the gravity loads shown in Fig. 13. The structure supports specified loads of 110 kN/m on floor beams B1 and B2 and 51 kN/m on roof beams B3 and B4, where the factored loads are 1.4 times the corresponding specified loads. F_y=248 MPa and $F_r=0.3F_y$.

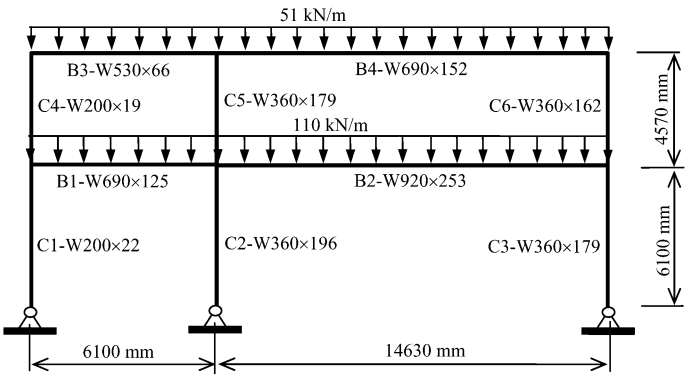

Fig. 13 Two-story moment frame

For the nonlinear analysis of this example, each column is represented by two elements while each beam is represented by four elements. The distributed loads are lumped at nodal points. Equations 18 to 21 are used to establish the θ_{pu}-κ relationship. The analysis terminated when the frame failed at load ratio λ=1.09. The lateral displacement of the top right corner of the frame during the loading history is described by the continuous line in Fig. 14. The analysis results are in close agreement with those from other researchers.

Conclusions

This paper presents a nonlinear analysis method for steel frames using a new plastic-hinge model. Two separate parameters are used in the hinge model to mimic the spread of plasticity both through section depth and along member length respectively. The proposed plastic-hinge model is general and applicable to all kinds of beam-columns, while specific numerical examples were conducted for steel frames with wide flange I-sections. The method is simple to implement since it only involves the

modification of a conventional elastic matrix displacement procedure. Numerical examples demonstrated the accuracy of the proposed analysis method.

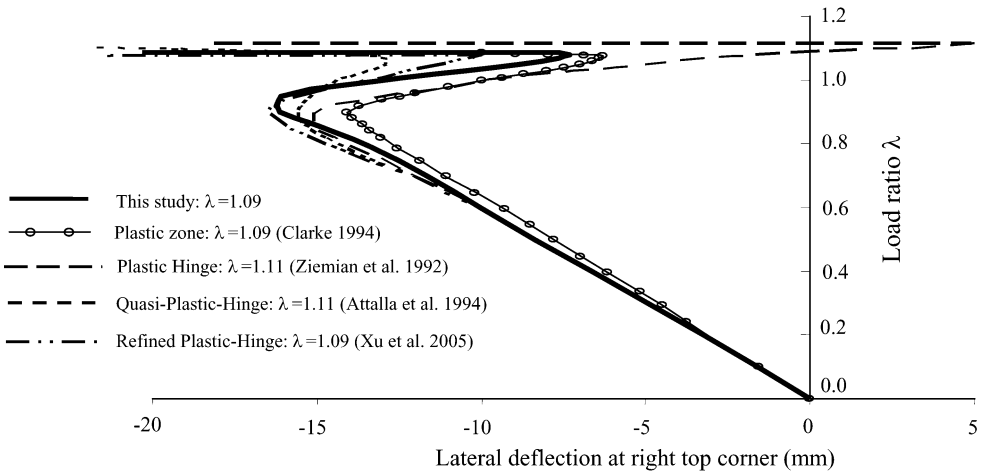

Fig. 14 Lateral deflection of the moment frame

References

Attalla, M.R., Deierlein, G.G., and McGuire, W. 1994. Spread of plasticity: quasi-plastic-hinge approach. Journal of Structural Engineering, ASCE, **120**(8): 2451-2473.

Chen, W.F. 1971. Further studies of inelastic beam-column problem. Journal of the Structural Division, ASCE, **97**(2): 529-544.

Chen, W.F, and Chan, S.L. 1995. Second-order inelastic analysis of steel frames using element with midspan and end springs. Journal of Structural Engineering, **121**(3): 530-541.

Chen, W.F., and Toma, S. 1994. Advanced analysis of steel frames. CRC Press, Boca Raton.

CISC. 2004. Handbook of steel construction, 8th Edition. Canadian Institute of Steel Construction.

Clarke, M.J. 1994. Chapter 6: plastic-zone analysis of frames. In: Chen, W.F., and Toma, S, editors. Advanced analysis of steel frames. CRC Press.

Duan, L., and Chen, W.F. 1990. A yield surface equation for doubly symmetrical sections. Engineering Structures, **12**(2): 114-119.

Hasan, R., Xu, L., and Grierson, D.E. 2002. Push-over analysis for performance-based seismic design. Computer and Structures, **80**: 2483–2493.

Lay, M.G., and Galambos, T.V. 1964. Tests on beam and column subassemblages. Frits Engineering Laboratory Report No. 278.10, Lehigh University.

Liew, J.Y.R., White, D.W., and Chen, W.F. 1993. Second-order refined plastic-hinge analysis for frame design. Part I. Journal of Structural Engineering, ASCE, **119**(11): 3196-3216.

Xu, L. 2001. Second-order analysis for semirigid steel frame design. Canadian Journal of Civil Engineering, **28**: 59-76.

Xu, L., and Liu, Y. 2005. Nonlinear analysis of inelastic steel frames. Proceedings of the 4th International Conference on Advances in Steel Structures, June 13-15, Shanghai, China.

Xu, L., Liu, Y., and Grierson, D.E. 2005. Nonlinear analysis of steel frameworks through direct modification of member stiffness properties. Advances in Engineering Software, **36**: 312-324.

Ziemian, R.D., McGuire, W., and Deierlein, G.G. 1992. Inelastic limit states design part I: planar frame structures. Journal of Structural Engineering, ASCE, **118**(9): 2532–49.